Journal of Materials Chemistry C

Accepted Manuscript

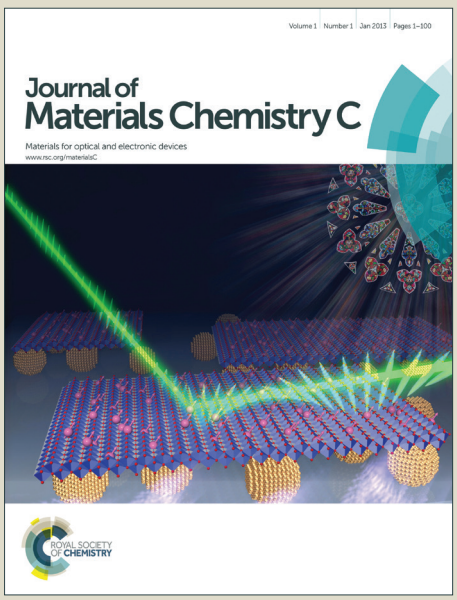

ROYAL SOCIETY OF CHEMISTRY

www.rsc.org/materialsC

Journal Name

RSCPublishing

COMMUNICATION

Preparation of a Novel Red $Rb_2SiF_6:Mn^{4+}$ Phosphor with High Thermal Stability through a Simple One-step Approach

Mu-Huai Fang,[a] Hoang-Duy Nguyen,[a,b] Chun Che Lin,[a] and Ru-Shi Liu [*a,c]

Print / Print SetupCopy to Clipboard as MetafilCopy to Clipboard as BitmapCite this: DOI: 10.1039/x0xx00000x

Received 00th January 2012,
Accepted 00th January 2012

DOI: 10.1039/x0xx00000x

www.rsc.org/

A new $Rb_2SiF_6:Mn^{4+}$ phosphor has been successfully synthesized through a one-step co-precipitation method. The addition of H_2O_2 into the solution with appropriate reaction temperature results in the reduction of Mn^{7+} into Mn^{4+}. Mn^{4+} is excited by UV and blue light, providing sharp red emission at approximately 630 nm. $Rb_2SiF_6:Mn^{4+}$ has a $Fm\bar{3}m$ (225) cubic phase crystal structure as determined using X-ray diffraction and Total Pattern Analysis Solutions. No apparent impurity phase is found in the X-ray diffraction spectrum. All luminescence properties, namely, emission, excitation, and thermal luminescent spectrum, have been deeply investigated.

1. Introduction

Illumination plays an important role in the progress of human history. Given their unique characteristics, white light-emitting diodes (WLEDs) have been extensively used in recent illumination systems. Compared with traditional illumination systems, LEDs are more efficient, more environment friendly, and longer lasting (more than 100,000 h), among others.[1–5] Phosphors have been broadly investigated as raw materials for LEDs. The most common LED is produced by combining the yellow phosphor $Y_3Al_5O_{12}:Ce^{3+}$ ($YAG:Ce^{3+}$) with blue LED chip. In spite of its low cost and easy fabrication, this LED still has several limitations. In particular, this material has low color rendering index ($Ra < 80$) and high correlated color temperature ($CCT > 6000$ K) because of the short red emission region in its spectrum. Therefore, some rare-earth metal-doped red phosphors, such as $CaAlSiN_3:Eu^{2+}$ and $Sr_2Si_5N_8:Eu^{2+}$ phosphors, are added into the device to enhance the color rendering index.[6,7] However, their broad emission band, which is longer than 650 nm, may decrease the efficiency of the device and the sensitivity of human eye. Numerous Mn^{4+}-doped red phosphors, such as $CaAl_{12}O_{19}:Mn^{4+}$, $YAlO_3:Mn^{4+}$, and $Sr_4Al_{14}O_{25}:Mn^{4+}$, have been investigated.[8–10] Contrary to the parity-forbidden *f-f* transition of rare-earth metals, the emission wavelength of *d-d* transition of transition metals is easily influenced by various coordinated environmental factors. Recently, Mn^{4+}-doped hexafluorosilicate phosphors, namely, $A_2SiF_6:Mn^{4+}$ (A = Na, K, Cs) and $BSiF_6:Mn^{4+}$ (B = Ba, Zn), have attracted considerable attention. Given its extremely high emission intensity and unique red line-emission spectrum, red light not only enhances the color rendering index of the device but also penetrates through the color filter of the back-lighting device. However, the Mn ion is highly sensitive to reaction conditions, such as temperature, because of its multiple valance states (2^+, 3^+, 4^+, 6^+, and 7^+). Therefore, controlling the valance state to yield Mn^{4+} is difficult. Adachia *et al.*[11–13] synthesized a series of $A_2MF_6:Mn^{4+}$ phosphors through wet chemical etching by mixing all precursors and silicon wafer into an HF solution. Pan *et al.*[14–16] synthesized $A_2MF_6:Mn^{4+}$ phosphors through hydrothermal reaction at approximately 120 °C. Nevertheless, both techniques have some drawbacks. High-purity phosphor is difficult to obtain by scratching the product on the surface of the silicon wafer. Furthermore, the working temperature of hydrothermal method is extremely high because of the high temperature sensitivity of Mn ion, leading to low Mn^{4+} concentration. In 2014, Zhu *et al.*[17] successfully synthesized $K_2TiF_6:Mn^{4+}$ through a co-precipitation method. They first synthesized K_2MnF_6 and then mixed it with the precursor in hydrofluoric acid. This two-step method provides high thermal stability, favorable crystallinity, and extremely high emission intensity. To the best of our knowledge, synthesizing A_2MnF_6 (A = Na, Rb, Cs) is difficult. Although K_2MnF_6 can be used to synthesize hexafluorosilicate phosphors, residual K ion should be found in the product.

In this study, a new $Rb_2SiF_6:Mn^{4+}$ phosphor was synthesized through a simple co-precipitation method. The product possesses red line-emission spectrum, high thermal stability, and high color purity. Hence, the prepared $Rb_2SiF_6:Mn^{4+}$ phosphor may have the potential to enhance the color rendering index of an LED device.

2. Experimental and characterizations

$Rb_2SiF_6:Mn^{4+}$ was synthesized through a one-step co-precipitation method, and the product is shown in Fig. 1.[18] Solution A was prepared by dissolving 0.8 g of SiO_2 into 15 mL of a 48% HF solution at approximately 70 °C for 1 h. Then, SiO_2 was dissolved, and the solution was cooled to room temperature. Solution B was prepared by dissolving 2.344 g of $RbMnO_4$ and 4.16 g of RbF into 15 mL of 48% HF for 1 h. Solutions A and B were vigorously stirred. Then, 1 mL of H_2O_2 was added into the mixed solution and stirred for 10 min. The color of the solution changed from dark purple into pink, and some powder precipitated at the bottom of the beaker. To obtain a high-purity product, the solution was dropped, and the powder was washed twice with 10 mL of 20% HF and thrice with 99% acetone. Finally, the powder was placed in an oven at 60 °C for 3 h, and the $Rb_2SiF:Mn^{4+}$ powder was obtained.

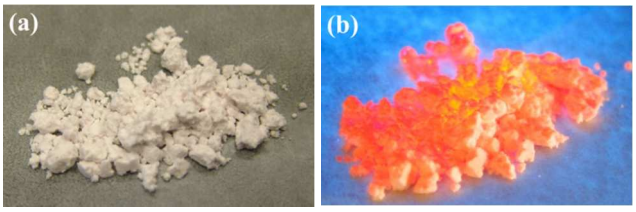

Fig. 1 Prepared $Rb_2SiF_6:Mn^{4+}$ phosphor under (a) room light and (b) 365 nm UV light excitation

The $Rb_2SiF_6:Mn^{4+}$ phosphor was synthesized through co-precipitation, with high-purity RbF (Alfa Aesar, Shanghai, China, 99.7%), $RbMnO_4$ (City Chemical LLC, America, 99%), SiO_2 (Aldrich, Shanghai, China, 99.997%), HF (Aldrich, Shanghai, China, 48%), and H_2O_2 (Aldrich, Shanghai, China, 34.5%–36.5%) as the raw materials. The sample was finely milled before the measurement. The structure of the sample was determined through X-ray diffraction (XRD) on a D2 Phaser diffractometer with CuKα radiation (Bruker). XRD data were collected from 10° to 100° (2θ) for approximately 6 h. The Rietveld refinement was analyzed using the Total Pattern Analysis Solutions software. The photoluminescence properties were measured using a 150 W Xe lamp and a Hamamatsu R928 photomultiplier tube equipped with a FluoroMax-3 spectrophotometer (HORIBA, Japan). The thermal stability from 25 °C to 300 °C was also tested using a FluoroMax-3 spectrophotometer and a heater (THMS-600) for temperature control.

3. Results and discussion

Structural analysis

The XRD refinement pattern is shown in Fig. 2(a). The peaks are well fitted and can be indexed to cubic crystal (JCPDS No. 00-007-0207). Its space group belongs to $Fm\bar{3}m$ (225), and no secondary phase is found in the pattern. Only a slight change in the peak symmetry occurs, especially for the peak at 2θ = 36.8° (2 2 2), which indicates a slight crystal distortion after Mn^{4+} doping. The crystal structure of Rb_2SiF_6 is shown in Fig. 2(b). The Si^{4+} ions are at the corner and the center face of the face-centered cubic (FCC) unit cell, which is also surrounded by six F^- ions with a hexagonal structure of SiF_6^{2-}. The Mn^{4+} ions are doped at the Si^{4+} positions, and they form the MnF_6^{2-} ion group. The Rb^+ ions occupy the eight tetragonal sites in the FCC structure.

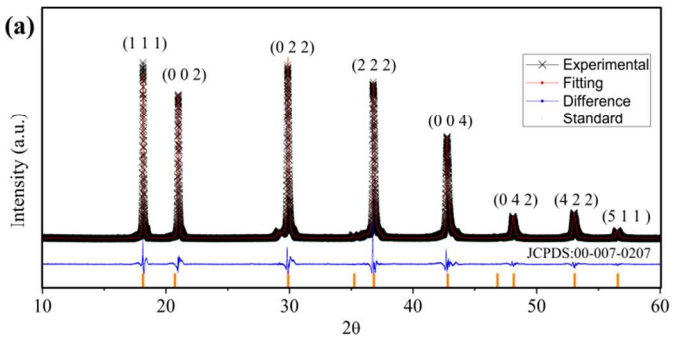

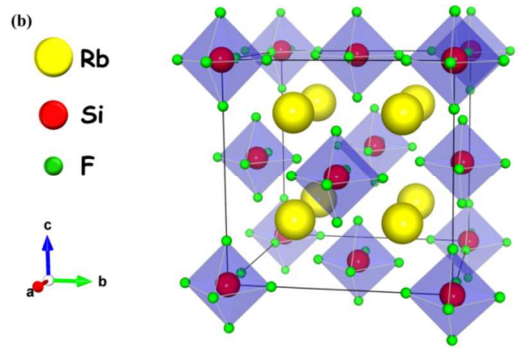

Fig. 2 (a) Rietveld refinement data and (b) crystal structure of $Rb_2SiF_6:Mn^{4+}$

Table 1 Crystal parameters from X-ray Rietveld refinements of $Rb_2SiF_6:Mn^{4+}$

Atoms	x	y	z	Frac	Beq
Rb	0.25000	0.25000	0.25000	1	2.521(16)
Si	0.00000	0.00000	0.00000	0.9852(61)	1.614(57)
Mn	0.00000	0.00000	0.00000	0.0148(61)	1.614(57)
F	0.19820(15)	0.00000	0.00000	1	2.336(39)
Space group	$Fm\bar{3}m$				
Cell Parameters	a = b = c = 8.45224(41) Å α = β = γ = 90° V = 603.832(87) Å^3				
Reliability Factors	χ^2 = 1.96 R_{wp} = 11.43% R_p = 8.35 %				

The morphology of $Rb_2SiF_6:Mn^{4+}$ is observed through scanning electron microscopy [Figs. 3(a) and 3(b)]. The particle size is between 5 and 20 μm. Some clear edges and corners are observed on the surface of the particle. These results indicate that the precursor has been well crystallized.

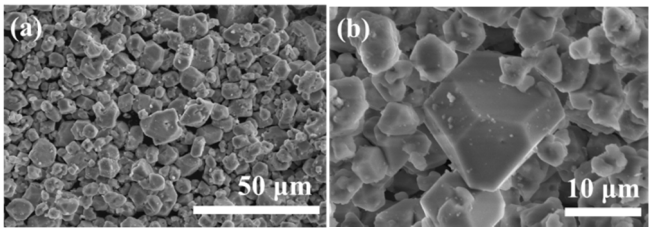

Fig. 3 Scanning electron micrograph of $Rb_2SiF_6:Mn^{4+}$

The Photoluminescence (PL) and Photoluminescence excitation (PLE) spectra measured at room temperature are shown in Fig. 4(a). The excitation spectrum is composed of two broad peaks. They spin-allow the transition from $^4A_{2g}$ to $^4T_{1g}$ and $^4A_{2g}$ to $^4T_{2g}$, which are

provided with absorption wavelengths at approximately 350 and 450 nm, respectively. According to the Tanabe–Sugano energy-level diagram shown in Fig. 4(c), the excitation peak position is largely affected by different levels of crystal field strength. Compared with GeF_6^{2-}, SiF_6^{2-} possesses stronger crystal field strength and hence shorter excitation wavelength[19]. The emission spectrum is shown in Fig. 4(b). Contrary to the excitation spectrum, the emission spectrum belongs to the spin-forbidden *d-d* transition from ^2E_g to $^4A_{2g}$. However, on the basis of the d^3 correlation diagram shown in Fig. 4(d), ^2E_g and $^4A_{2g}$ are provided with the same electron configuration as that of t_{2g}^3 but with different spin multiplicities of 2 and 4, respectively. The relative energy is only slightly related to the crystal field strength. Therefore, the energy of the emission peaks does not remarkably change with increasing ligand field strength. The three peaks longer than 620 nm belong to stoke ν_6 (t_{2u} bending), ν_4 (t_{1u} bending), and ν_3 (t_{1u} stretching) peaks, whereas the two peaks shorter than 620 nm belong to anti-stoke ν_6 (t_{2u} bending) and ν_4 (t_{1u} bending) peaks. In general, the zero-phonon line (ZPL) is at approximately 620 nm. However, the more symmetrical the coordination environment is, the weaker is the intensity of the ZPL line. The ZPL line at approximately 620 nm is difficult to observe because of the highly symmetrical environment of the Rb_2SiF_6:Mn^{4+} crystal.[20] In addition, the energy of ^2E_g is only affected by the spin flip; thus, its energy does not remarkably change with different levels of crystal field strength. Therefore, the emission wavelengths among various Mn^{4+}-doped hexa-fluoro phosphors are similar.

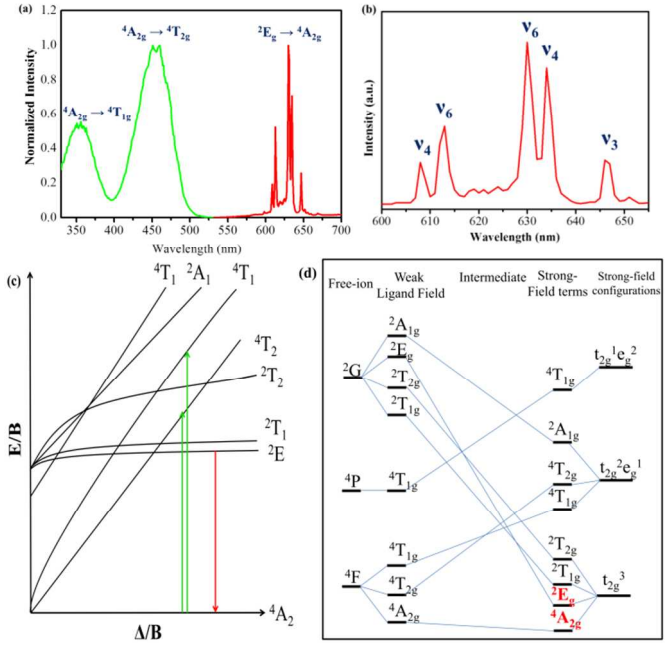

Fig. 4 (a) Normalized PL and PLE spectra of Rb_2SiF_6:Mn^{4+}; (b) PL spectrum of Rb_2SiF_6:Mn^{4+}; (c) Tanabe–Sugano energy-level diagram for d^3 ions in the octahedral coordinate environment; and (d) correlation diagram of d^3 ions in the octahedral coordinate environment.

The temperature-dependent thermal luminescent spectrum of Rb_2SiF_6:Mn^{4+} is shown in Fig. 5(a). No emission peak position shift is found when the temperature increases. The peak intensity decreases when the temperature increases. Nevertheless, the Mn^{4+} emission spectrum belongs to sharp line spectrum. The integrated spectrum area rather than the peak intensity should be considered when examining the thermal stability of Rb_2SiF_6:Mn^{4+}. Fig. 5(b) shows the excellent thermal stability of Rb_2SiF_6:Mn^{4+} in the temperature range of 25–300 °C. At 250 °C, the relative PL intensity of the sample remained over 100% compared with that at 25 °C, clearly showing better thermal stability than the widely used YAG:Ce phosphor (88% at 200 °C).[21] The integrated PL intensity of Rb_2SiF_6:Mn^{4+} decreases at 300 °C (70%) but is still higher than that of K_2SiF_6:Mn^{4+} (50%) or K_2TiF_6:Mn^{4+} (20%). The simple one-step synthesis and the obtained good thermal stability confirm that Rb_2SiF_6:Mn^{4+} red emitting phosphor is a prospective candidate for improving the color reproducibility of WLEDs.

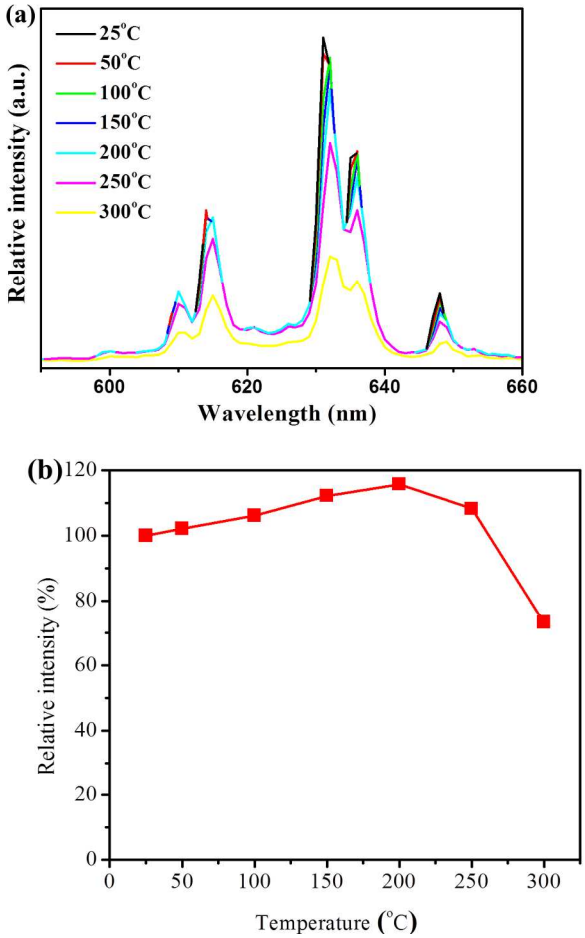

Fig. 5 (a) Temperature-dependent thermal luminescent spectrum of Rb_2SiF_6:Mn^{4+} phosphor and (b) relative intensity of emission spectrum by integrating the spectral area

In order to realize the emission decay property of the Rb_2SiF_6:Mn^{4+}, the room temperature PL decay curve from ^2E_g to $^4A_{2g}$ state is shown in Fig. 6. The decay time of the prepared phosphor is around 8.26 ms, which is fitted from a single exponential curve. Different with the *f-d* transition, the decay time for the *d-d* transition of Mn^{4+} ion will be much longer and in the range of mini seconds.

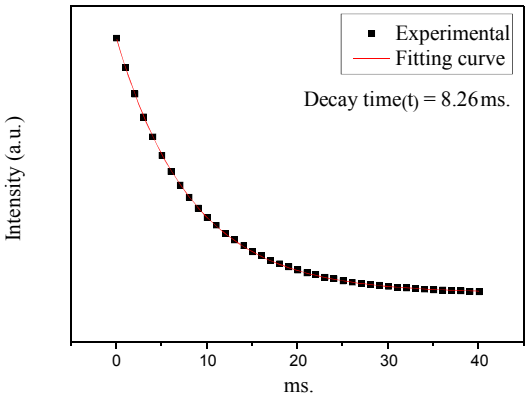

Fig. 6 Room temperature PL decay curves of $Rb_2SiF_6:Mn^{4+}$

4. Conclusions

A new phosphor, $Rb_2SiF_6:Mn^{4+}$, has been successfully synthesized through a one-step co-precipitation method. The phosphor has a cubic $Fm\bar{3}m$ crystal structure, and no impurities or second phases are discovered through XRD. $Rb_2SiF_6:Mn^{4+}$ is provided with blue light absorption and strong red line-emission. In addition, $Rb_2SiF_6:Mn^{4+}$ has good thermal stability, which is approximately 115% of the integrated spectrum area at 150 ℃ compared with that at room temperature. The morphology of the phosphor is also examined via scanning electron microscopy. $Rb_2SiF_6:Mn^{4+}$ is well crystallized with particle sizes ranging from 5 μm to 20 μm. This phosphor could be a promising material for WLEDs.

Acknowledgements

The authors would like to thank the Ministry of Science and Technology of Taiwan (Contract Nos. MOST 101-2113-M-002-014-MY3) for financially supporting this study. The financial support from the Industrial Technology Research Institute (Contract No. D351A41300) is also appreciated.

Notes and references

[a] Department of Chemistry, National Taiwan University, Taipei 106, Taiwan
[b]Institute of Applied Material Science, Vietnam Academy of Science and Technology, Hochiminh City, Vietnam
[c]Department of Mechanical Engineering and Graduate Institute of Manufacturing Technology, National Taipei University of Technology, Taipei 106, Taiwan

1 W. T. Chen; H. S. Sheu; R. S. Liu; J. P. Attfield, *J. Am. Chem. Soc.* 2012**, 134**, 8022-8025.
2 W. B. Park, Singh, S. P., Yoon, C. & Sohn, K. S. , *J. Mater. Chem. C* 2013**, 1**, 1832-1839.
3 H. Daicho; T. Iwasaki; K. Enomoto; Y. Sasaki; Y. Maeno; Y. Shinomiya; S. Aoyagi; E. Nishibori; M. Sakata; H. Sawa; S. Matsuishi; H. Hosono, *Nat. Commun.* 2012**, 3**, 1132.
4 C. Y. Sun; X. L. Wang; X. Zhang; C. Qin; P. Li; Z. M. Su; D. X. Zhu; G. G. Shan; K. Z. Shao; H. Wu; J. Li, *Nat Commun* 2013**, 4**, 2717.
5 C. W. Yeh; W. T. Chen; R. S. Liu; S. F. Hu; H. S. Sheu; J. M. Chen; H. T. Hintzen, *J. Am. Chem. Soc.* 2012**, 134**, 14108-14117.
6 X. Q. Piao; T. Horikawa; H. Hanzawa; K. Machida, *Appl. Phys. Lett.* 2006**, 88**, 161908.
7 K. Uheda; N. Hirosaki; Y. Yamamoto; A. Naito; T. Nakajima; H. Yamamoto, *Electrochem. Solid-State Lett.* 2006**, 9**, H22-H25.
8 T. Murata; T. Tanoue; M. Iwasaki; K. Morinaga; T. Hase, *J. Lumines.* 2005**, 114**, 207-212.
9 Y. Zhydachevskii; D. Galanciak; S. Kobyakov; M. Berkowski; A. Kaminska; A. Suchocki; Y. Zakharko; A. Durygin, *J. Phys.-Condes. Matter* 2006**, 18**, 11385-11396.
10 M. Y. Peng; X. W. Yin; P. A. Tanner; C. Q. Liang; P. F. Li; Q. Y. Zhang; J. R. Qiu, *J. Am. Ceram. Soc.* 2013**, 96**, 2870-2876.
11 S. Adachi; T. Takahashi, *J. Appl. Phys.* 2008**, 104**, 023512/1-023512/3.
12 T. Arai; Y. Arai; T. Takahashi; S. Adachi, *J. Appl. Phys.* 2010**, 108**, 063506/1-063506/7.
13 D. Sekiguchi; S. Adachi, *ECS J. Solid State Sci. Technol.* 2014**, 3**, R60-R64.
14 X. Y. Jiang; Y. X. Pan; S. M. Huang; X. Chen; J. G. Wang; G. K. Liu, *J. Mater. Chem. C* 2014**, 2**, 2301-2306.
15 L. F. Lv; X. Y. Jiang; S. M. Huang; X. Chen; Y. X. Pan, *J. Mater. Chem. C* 2014**, 2**, 3879-3884.
16 L. F. Lv; X. Y. Jiang; Y. X. Pan; G. K. Liu; S. M. Huang, *J. Lumines.* 2014**, 152**, 214-217.
17 H. M. Zhu; C. C. Lin; W. Q. Luo; S. T. Shu; Z. G. Liu; Y. S. Liu; J. T. Kong; E. Ma; Y. G. Cao; R. S. Liu; X. Y. Chen, *Nat. Commun.* 2014**, 5**, 4312.
18 H. D. Nguyen; C. C. Lin; M. H. Fang; R. S. Liu, *J. Mater. Chem. C* 2014**, 2**, 10268-10272.
19 L. L. Wei; C. C. Lin; M. H. Fang; M. G. Brik; S. F. Hu; H. Jiao; R. S. Liu, *J. Mater. Chem. C* 2015**, 3**, 1655-1660.
20 R. Kasa; S. Adachi, *J. Electrochem. Soc.* 2012**, 159**, J89-J95.
21 H. L. Q. Shao, Y. Dong, J. Jiang, C. Liang, J. He, *J. Alloy. Compd.* 2010**, 498**, 199.